
UniTriGen: Unified Triplet Generation of Aligned Visible-Infrared-Label for Few-Shot RGB-T Semantic Segmentation

Ping Zhou¹ Haoyu Wang¹ Mengmeng Zheng¹ Lei Zhang^{1,*}
Wei Wei¹ Chen Ding² Fei Zhou³

¹School of Computer Science, Northwestern Polytechnical University

²School of Computer Science & Technology, Xi'an University of Posts & Telecommunications

³MMLab, The Chinese University of Hong Kong

zhou_ping@mail.nwpu.edu.cn nwpuzhanglei@nwpu.edu.cn

*Corresponding authors.

Abstract

RGB-T semantic segmentation requires strictly aligned VIS-IR-Label triplets; however, such aligned triplet data are often scarce in real-world scenarios. Existing generative augmentation methods usually adopt cascaded generation paradigms, decomposing joint triplet generation into local conditional processes. As a result, consistency among VIS, IR, and Label in spatial structure, semantic content, and cross-modal details cannot be reliably maintained. To address this issue, we propose UniTriGen, a unified triplet generation framework that directly generates spatially aligned, semantically consistent, and modality complementary VIS-IR-Label triplets under the guidance of text prompts. UniTriGen first introduces a unified triplet generation mechanism, where VIS, IR, and Label are jointly encoded into a shared latent space and modeled with a diffusion process to enforce global cross-modal consistency. Lightweight modality-specific residual adapters are further integrated into this mechanism to accommodate modality-specific imaging characteristics and output formats. To mitigate generation bias caused by imbalanced scene and class distributions in limited paired triplets, UniTriGen also employs a scene-balanced and class-aware few-shot sampling strategy, which induces a more balanced sampling distribution and enhances the scene and class diversity of generated triplets. Experiments show that UniTriGen generates high-quality aligned triplets from limited real paired data, thereby achieving consistent performance improvements across various RGB-T semantic segmentation models.

1 Introduction

For RGB-T semantic segmentation, effective training samples should consist of strictly aligned same-scene Visible-Infrared-Label (VIS-IR-Label) triplets. The three modalities must share consistent scene layouts, object locations, boundaries, and semantic classes, so that visible appearance, infrared thermal responses, and pixel-level semantic supervision correspond within a common spatial coordinate frame. However, due to the practical challenges of multi-sensor acquisition, accurate cross-modal registration, and pixel-level semantic annotation, real RGB-T datasets typically provide only a small number of aligned and annotated triplets. Consequently, learning with only a limited number of paired triplets as training data becomes a more realistic yet more challenging setting.

A natural solution to this limitation is to use generative models to synthesize additional training triplets. However, this task is fundamentally different from generating each modality independently. Since VIS, IR, and Label are heterogeneous dense representations of the same scene, the generated triplets must preserve shared spatial structures, consistent semantic regions, and complementary cross-modal information. Therefore, the key challenge is not merely to generate more samples, but to

learn the joint generative distribution of VIS, IR, and Label under the same scene from limited paired triplets.

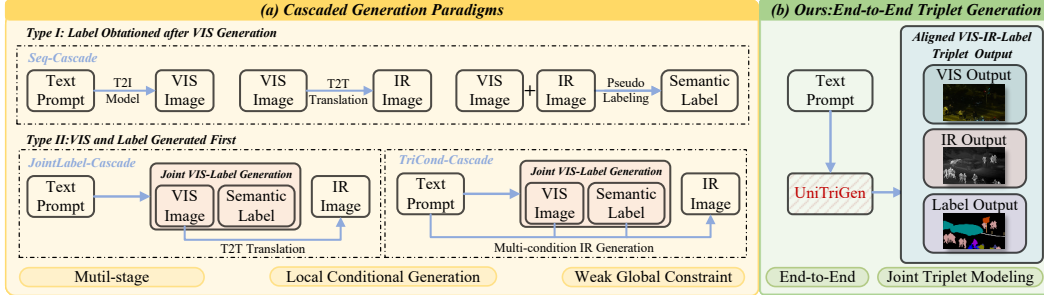


Figure 1: Comparison between existing paradigms and the proposed UniTriGen. (a) Cascaded Generation Paradigms that progressively assemble the target triplet through intermediate outputs. (b) Our UniTriGen directly generates spatially aligned, semantically consistent, and modality complementary VIS-IR-Label triplets from text prompts in an end-to-end manner.

To the best of our knowledge, text-driven generation of aligned VIS-IR-Label triplets has not yet been directly explored. Although existing generative paradigms can be adapted as alternatives, most follow cascaded generation paradigms. As shown in Figure 1(a), Seq-Cascade first generates visible images, then translates them into infrared images, and predicts the semantic labels. JointLabel-Cascade and TriCond-Cascade first generate image-label pairs and then synthesize the missing infrared images. Although these methods can produce triplets in form, they essentially decompose the target joint distribution into multiple local conditional generation processes. Specifically, each stage generates the next modality conditioned solely on the output of the preceding stage. Unlike a unified generation process that jointly constrains VIS, IR, and Label, this sequential design may propagate inconsistencies across stages. As a result, even if the output of each individual stage appears plausible, the final triplet may still suffer from layout shifts, boundary inconsistencies, semantic region mismatches, and cross-modal detail conflicts. In other words, cascaded paradigms are limited not only by error propagation and amplification along the generation chain, but also, more fundamentally, by their inability to impose global and unified cross-modal consistency constraints on the three modalities.

To address the above challenges, as shown in Figure 1(b), we propose **UniTriGen**, a **Unified Triplet Generation** framework that directly generates spatially aligned, semantically consistent, and modality-complementary VIS-IR-Label triplets under the guidance of text prompts. Specifically, a unified triplet generation mechanism is first designed (Section 3.2), in which VIS images, IR images, and semantic labels are jointly encoded into a shared latent space. The resulting concatenated triplet latent representation is then modeled by a diffusion model, thereby explicitly enforcing cross-modal consistency among the three modalities. To account for the substantial differences among VIS, IR, and Label in imaging characteristics and decoding objectives, lightweight modality-specific residual adapters are further introduced during triplet decoding. These adapters improve modality-specific fidelity while preserving cross-modal consistency. In addition, when learning from only a limited number of paired triplets, the training data often exhibit highly imbalanced distributions of scenes and classes. This imbalance can bias the generative model toward frequent scenes and common classes, making it difficult to generate low-frequency scenes and rare classes. To mitigate this generation bias, a scene-balanced and class-aware few-shot sampling strategy is proposed (Section 3.3). By constructing structured scene-class prompts, introducing explicit scene encoding, and applying hierarchical resampling, this strategy induces more balanced sampling distributions over scenes and classes. Consequently, the model’s dependence on frequent scenes and common classes is reduced, and the scene and class diversity of generated triplets is enhanced. With these designs, UniTriGen can generate many high-quality aligned VIS-IR-Label triplets using only a small number of real paired triplets, thereby improving the training of downstream RGB-T semantic segmentation models. Our main contributions are summarized as follows:

- We propose UniTriGen, a text-to-VIS-IR-Label aligned triplet generation framework. The unified triplet generation mechanism jointly models VIS, IR, and Label in a shared latent space and employs lightweight modality-specific residual adapters for triplet decoding,

producing spatially aligned, semantically consistent, and modality complementary triplets with improved modality fidelity and cross-modal consistency.

- We design a scene-balanced and class-aware few-shot sampling strategy that integrates structured scene-class prompts, explicit scene encoding, and hierarchical resampling to reduce bias toward frequent scenes and common classes, thereby enhancing the diversity of generated triplets across scenes and classes.
- We conduct extensive experiments on SemanticRT and PST900. Results show that the high-quality synthetic triplets generated by UniTriGen effectively improve existing RGB-T semantic segmentation models and exhibit strong transferability across downstream architectures and data settings.

2 Related Works

2.1 Dataset Generation for Semantic Segmentation

Data generation for semantic segmentation[1][2][3][4][5][6] has recently attracted increasing attention as a task-oriented data synthesis strategy. Unlike generic image synthesis[7][8][9][10][11], this line of work aims to produce training samples that improve pixel-level recognition rather than merely enhance visual realism. Existing methods can be broadly categorized according to how semantic supervision is obtained during generation, including Image-to-Mask, Mask-to-Image, and Image-Mask joint generation. In Image-to-Mask pipelines[12][4][13], images are first generated or augmented, and semantic masks are subsequently obtained through segmentation models, pseudo-labeling strategies, or foundation-model-assisted annotation[14][15]. These methods are flexible and can benefit from powerful generative models, but their label quality is bound by the reliability of the subsequent mask prediction stage. In contrast, Mask-to-Image methods[16][17] synthesize images conditioned on given semantic layouts or class masks. This paradigm provides explicit control over spatial structures and class compositions, but typically relies on existing masks and mainly diversifies visual appearance under fixed label structures, thereby limiting scene-level diversity. More recently, Image-Mask joint generation methods[6][18] attempt to synthesize images and their corresponding semantic labels simultaneously through shared latent modeling or coupled optimization objectives. For example, JoDiffusion[6] introduces a text-prompt-driven joint generation framework for images and pixel-wise semantic labels, where a unified latent space, joint diffusion process, and mask refinement strategy are employed to synthesize diverse and highly consistent image-label pairs. Since image content and pixel-wise labels can be constrained within a unified generation process, joint generation is better suited to segmentation-oriented data augmentation. Nevertheless, most existing semantic dataset generation methods remain designed for image-label pairs, especially in the visible domain, with limited consideration of heterogeneous sensing modalities such as infrared imagery.

2.2 Visible-to-Infrared Image Translation

Visible-to-infrared image translation[19][20][21] aims to synthesize infrared images from visible images, thereby alleviating the scarcity of thermal data and expanding modality availability for multimodal perception. Early studies commonly formulate this task as image-to-image translation and learn cross-domain mappings through Variational Autoencoders (VAEs)[22][23] or Generative Adversarial Networks (GANs)[22][24][25][26]. To better preserve scene structures during modality transfer, subsequent methods introduce additional constraints such as edge guidance[27], structural similarity[28], representation learning[29], or multi-scale feature alignment[30]. More recently, diffusion-based[31][19][32] and conditional generative methods[33] have further improved infrared synthesis by leveraging stronger generative priors to model the target infrared distribution. These studies demonstrate the feasibility of synthesizing infrared-like images from visible observations and provide useful tools for modality expansion. However, most existing visible-to-infrared translation methods are essentially designed as bimodal mapping models. They usually focus on generating visually plausible infrared images, while their effectiveness and direct usability for downstream tasks are rarely explicitly optimized.

To generate VIS-IR-Label training triplets for complex scenes, a straightforward strategy is to combine image-label generation with visible-to-infrared translation. Such a cascaded pipeline first synthesizes visible images and their semantic labels and then translates the visible images into the

infrared domain. However, this formulation decomposes triplet generation into loosely coupled local conditional processes, where the label and infrared modality are generated at different stages rather than being jointly constrained within a unified diffusion modeling process. As a result, the assembled triplets may suffer from spatial misalignment, semantic mismatch, boundary inconsistency, and cross-modal detail conflicts. This issue becomes more severe when learning from only a limited number of paired VIS-IR-Label triplets, since the scarce cross-modal correspondences make it difficult for independently trained modules to capture global cross-modal consistency. In contrast, UniTriGen treats VIS, IR, and Label as a unified generation target and models them within a single diffusion framework, enabling joint enforcement of spatial alignment, semantic consistency, and modality complementarity.

3 Methodology

3.1 Problem Setup

We investigate multi-source aligned triplet generation under a few-shot learning setting. Given a limited real paired dataset $\mathcal{D}_{real} = \{(V_i, I_i, L_i, T_i)\}_{i=1}^N$, where V_i , I_i , and L_i represent the visible image, infrared image, and semantic label from the same scene, respectively, and T_i denotes the corresponding text prompt. Our goal is to learn a text-conditioned triplet generation model $G_\theta : T \rightarrow (V, I, L)$, which can generate spatially aligned, semantically consistent, and modality complementary VIS-IR-Label triplets in an end-to-end manner solely from text prompts.

The synthetic dataset is denoted as $\mathcal{D}_{syn} = \{(\hat{V}_j, \hat{I}_j, \hat{L}_j)\}_{j=1}^{N_{syn}}$. These samples are expected to satisfy two fundamental requirements. First, the triplets outputs should exhibit strict consistency in scene layout, object locations, and class semantics. Second, the generated labels should be trainable and directly serve as supervision signals for downstream RGB-T semantic segmentation models. Therefore, the final objective is to expand the training set using limited real paired data in combination with a synthetic dataset ($\mathcal{D}_{real} \cup \mathcal{D}_{syn}$), thereby enhancing the performance of downstream RGB-T semantic segmentation models.

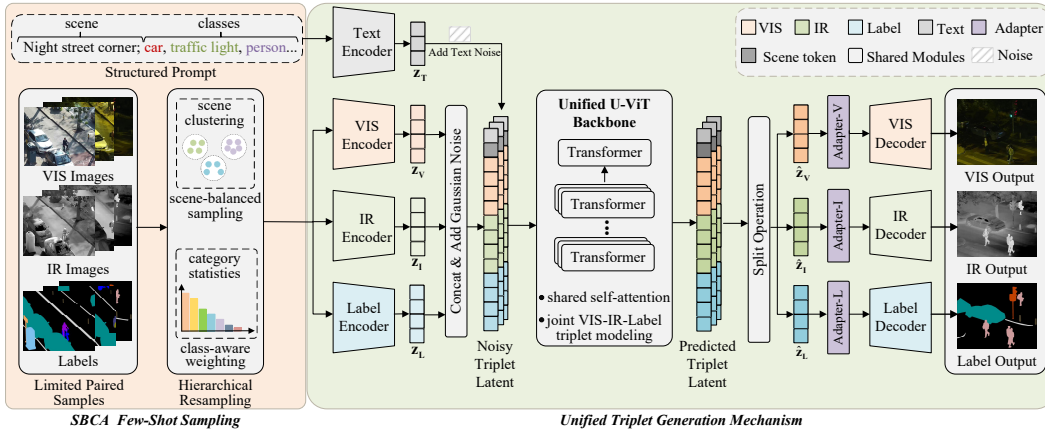


Figure 2: Overview of the UniTriGen framework. The framework consists of two main components: Unified Triplet Generation Mechanism and SBCA Few-Shot Sampling.

3.2 Unified Triplet Generation Mechanism

To enable end-to-end text-to-VIS-IR-Label Aligned triplet generation, we construct a **Unified Triplet Generation Mechanism** based on the UniDiffuser[34] architecture, which integrates joint cross-modal diffusion modeling and modality-specific latent calibration into a single generation process. The core idea is to first encode the visible image, infrared image, and semantic label into a shared latent space and jointly model them within a unified diffusion process, so that the three modalities can share scene-level structural and semantic constraints throughout generation. Then, before decoding, lightweight modality-specific residual adapters calibrate the predicted latents to better match the decoding characteristics of each modality. In this way, unified triplet generation simultaneously preserves cross-modal consistency and improves modality-dependent fidelity.

Joint triplet latent diffusion. Given a text prompt T , we employ the CLIP[15] text encoder \mathcal{E}_T to obtain the text latent representation $z_T = \mathcal{E}_T(T)$. For an aligned triplet (V, I, L) , we use modality-specific VAE encoders E_V , E_I , and E_L to encode the visible image, infrared image, and semantic label, respectively, and concatenate their latent variables into a unified triplet latent representation:

$$z_V = E_V(V), \quad z_I = E_I(I), \quad z_L = E_L(L), \quad z_0 = [z_V; z_I; z_L]. \quad (1)$$

This representation enables the model to capture visible appearance, infrared thermal cues, and label boundaries within a unified generation space, rather than treating them as independent targets.

In the forward diffusion process, Gaussian noise is injected into z_0 to obtain the noisy latent variable at timestep t :

$$q(z_t | z_0) = \mathcal{N}(\sqrt{\bar{\alpha}_t}z_0, (1 - \bar{\alpha}_t)\mathbf{I}), \quad z_t = \sqrt{\bar{\alpha}_t}z_0 + \sqrt{1 - \bar{\alpha}_t}\epsilon, \quad \epsilon \sim \mathcal{N}(0, \mathbf{I}). \quad (2)$$

This joint noising scheme encourages the network to learn spatial correspondence and semantic coupling across modalities.

During reverse denoising, the text latent z_T serves as the sole external condition and is fed together with the noisy triplet latent into a unified U-ViT backbone. Through self-attention over the unified token sequence, the network models interactions between text and the three modality-specific latent components and predicts the injected noise $\epsilon_\theta(z_t, z_T, t)$. The reverse transition is defined as

$$p_\theta(z_{t-1} | z_t, z_T) = \mathcal{N}(\mu_\theta(z_t, z_T, t), \sigma_t^2\mathbf{I}), \quad (3)$$

where the denoised mean is computed by

$$\mu_\theta(z_t, z_T, t) = \frac{1}{\sqrt{\alpha_t}} \left(z_t - \frac{1 - \alpha_t}{\sqrt{1 - \bar{\alpha}_t}} \epsilon_\theta(z_t, z_T, t) \right). \quad (4)$$

The baseline is optimized with the standard noise prediction objective:

$$\mathcal{L}_{\text{denoise}} = \mathbb{E}_{t, z_0, \epsilon} [\|\epsilon_\theta(z_t, z_T, t) - \epsilon\|_2^2]. \quad (5)$$

Modality-specific latent calibration. Although the unified diffusion backbone jointly models VIS, IR, and Label in a shared latent space, the three modalities have distinct decoding requirements. VIS emphasizes color, texture, and structural details; IR highlights thermal responses and salient contours; and Label requires discrete semantic regions with clear object boundaries. Therefore, directly feeding the backbone-predicted latents into their corresponding decoders may cause residual discrepancies between the predicted latents and the target modality-specific decoding manifolds.

To address this issue while preserving the unified generation process, we introduce lightweight modality-specific residual adapters after joint denoising and before triplet decoding. Inspired by Any2Any [32], each adapter performs a residual calibration on the corresponding predicted latent. We denote the predicted latent of modality m as \hat{z}_m , where $m \in \{V, I, L\}$. The calibrated latent is defined as:

$$\tilde{z}_m = \hat{z}_m + A_\phi^m(\hat{z}_m), \quad m \in \{V, I, L\}, \quad (6)$$

where A_ϕ^m denotes the lightweight adapter for modality m , and ϕ denotes its learnable parameters. The calibrated latents are then decoded by their corresponding modality decoders:

$$\hat{x}_m = D_m(\tilde{z}_m), \quad m \in \{V, I, L\}, \quad (7)$$

where \hat{x}_V , \hat{x}_I , and \hat{x}_L correspond to the generated visible image, infrared image, and semantic label, respectively. D_m denotes the decoder corresponding to modality m .

During training, the adapters are supervised in the latent space by encouraging the calibrated latent to approximate the corresponding ground-truth modality latent. To prevent the adapter loss from disturbing the unified diffusion backbone, stop-gradient is applied to the backbone-predicted latent when optimizing the adapters:

$$\mathcal{L}_{\text{calib}} = \sum_{m \in \{V, I, L\}} \left\| \text{sg}(\hat{z}_m) + A_\phi^m(\text{sg}(\hat{z}_m)) - z_m \right\|_2^2, \quad (8)$$

where $z_m = E_m(x_m)$ denotes the ground-truth latent of modality m , and $\text{sg}(\cdot)$ denotes the stop-gradient operation. The overall objective of unified triplet generation is:

$$\mathcal{L}_{\text{UTG}} = \mathcal{L}_{\text{denoise}} + \lambda \mathcal{L}_{\text{calib}}, \quad (9)$$

where λ balances joint triplet diffusion modeling and modality-specific latent calibration.

During inference, VIS, IR, and Label are first jointly generated through the unified reverse diffusion process. The denoised triplet latent is then calibrated once by the modality-specific adapters and decoded into the final triplet outputs. Since the adapters are only applied after denoising and do not participate in iterative diffusion sampling, they introduce negligible computational overhead. Overall, the unified triplet generation mechanism enables UniTriGen to produce spatially aligned, semantically consistent, and modality-complementary VIS-IR-Label triplets from text prompts within a single coherent generation process.

3.3 SBCA Few-Shot Sampling

When only a limited number of paired triplets are available for training, the training data often exhibit highly imbalanced scene and semantic class distributions. Such imbalance biases the generative model toward frequent scenes and common classes, leading to inadequate representation of low-frequency scenes and rare classes. Consequently, the diversity of the synthetic triplets is substantially limited. To mitigate this issue, we propose a **Scene-Balanced and Class-Aware (SBCA) Few-Shot Sampling** strategy, which induces more balanced sampling distributions over scenes and classes through structured text condition, explicit scene encoding, and hierarchical sample resampling.

Structured scene-class prompt. We structure the text prompt of each training sample into a scene-class format. Specifically, for each sample i , its text representation T_i is constructed as $[d_i^s; d_i^c]$, where d_i^s denotes the scene description and d_i^c denotes the set of semantic classes appearing in the sample. For example, a sample can be written as: *Nighttime parking area adjacent to a dense forest background; car, traffic light, pole, curve, person*. This format explicitly injects both global scene context and local object classes into the text condition, enabling the model to perceive scene background and object semantics simultaneously.

Explicit scene encoding. To disentangle scene semantics from class semantics in the text embedding space, we introduce explicit scene encoding. We first employ the Places365-CNNs [35] classification model to extract scene representations, and cluster the training set into K scene groups:

$$\mathcal{D}_{real} = \{\mathcal{G}_1, \mathcal{G}_2, \dots, \mathcal{G}_K\}. \quad (10)$$

For sample i , its scene identity is denoted as $s_i \in \{1, \dots, K\}$. During text encoding, we append a learnable scene token to the original text representation, giving the augmented text latent:

$$\tilde{z}_{T_i} = [\mathcal{E}_T(T_i); e_{s_i}], \quad (11)$$

where e_{s_i} is the learnable embedding of scene s_i . In practice, \tilde{z}_{T_i} replaces z_T as the text condition in unified triplet generation, allowing the diffusion backbone to receive both class-aware semantic prompts and explicit scene-level guidance.

Scene-balanced and class-aware resampling. During training, we implement a hierarchical resampling mechanism: first, balancing the overall sampling probability across scenes, and then weighting samples within each scene according to class rarity. For each class c , let N_c denote the number of training samples containing this class. If sample i belongs to scene group \mathcal{G}_k , its final sampling weight is defined as:

$$W_i = \frac{1}{K} \cdot \frac{r_i}{\sum_{j \in \mathcal{G}_k} r_j}, \quad \text{where } r_i = \epsilon + \max_{c \in \mathcal{C}_i} w_c, \quad w_c = \frac{1}{N_c^\alpha}. \quad (12)$$

Here, K denotes the number of scene groups, \mathcal{G}_k denotes the scene group to which sample i belongs, \mathcal{C}_i denotes the class set of sample i , α is a smoothing coefficient, and ϵ ensures a non-zero probability for every sample. This mechanism enhances supervision for tail scenes and classes, yielding a more balanced training distribution for VIS-IR-Label triplet generation.

4 Experiments and Results

4.1 Datasets and Experimental Settings

Datasets. We evaluate UniTriGen on two public RGB-T semantic segmentation datasets: **Semanti-cRT**[36] and **PST900**[37]. To simulate practical scenarios with limited paired triplet data, we conduct

Downstream Methods	Backbone	Augmentation Methods	5% SemanticRT Dataset			50% PST900 Dataset		
			Data Size (Pairs)	mIoU (Syn only)	mIoU (Real+Syn)	Data Size (Pairs)	mIoU (Syn only)	mIoU (Real+Syn)
SemanticRT[36]	ResNet152	Raw Data	342		66.62	299		78.51
		Seq-Cascade	684	41.81	71.59	598	39.87	79.76
		JointLabel-Cascade	684	43.22	71.78	598	35.77	78.10
		TriCond-Cascade	684	<u>50.76</u>	<u>73.02</u>	598	<u>40.83</u>	<u>81.95</u>
		UniTriGen (Ours)	684	54.16	73.12	598	41.39	83.96
M-SpecGene[39]	UperNet	Raw Data	342		69.38	299		74.96
		Seq-Cascade	684	43.19	70.71	598	49.41	75.50
		JointLabel-Cascade	684	43.63	70.99	598	49.17	76.00
		TriCond-Cascade	684	<u>51.79</u>	<u>71.17</u>	598	<u>49.46</u>	<u>76.76</u>
		UniTriGen (Ours)	684	58.90	71.57	598	65.48	79.31
Sigma[40]	Mamba	Raw Data	342		73.46	299		85.86
		Seq-Cascade	684	42.72	73.04	598	51.76	85.99
		JointLabel-Cascade	684	47.56	73.45	598	46.37	85.25
		TriCond-Cascade	684	<u>53.20</u>	<u>73.65</u>	598	<u>52.88</u>	<u>86.48</u>
		UniTriGen (Ours)	684	58.11	74.36	598	53.61	87.06
MilNet[41]	Segformer	Raw Data	342		69.73	299		86.42
		Seq-Cascade	684	40.90	69.92	598	54.50	85.34
		JointLabel-Cascade	684	48.70	70.70	598	47.80	84.30
		TriCond-Cascade	684	<u>55.60</u>	<u>71.02</u>	598	<u>55.60</u>	<u>85.37</u>
		UniTriGen (Ours)	684	57.30	71.45	598	64.90	87.29

Table 1: Quantitative comparison of different methods on SemanticRT and PST900 datasets. The best results are highlighted in **bold**, while the second-best outcomes are denoted by *underlined italic*.

experiments under a few-shot setting. Specifically, for **SemanticRT**, we sample **5%** of the dataset, resulting in 342 training samples, 85 validation samples, and 142 testing samples. For **PST900**, we use **50%** of the dataset, with 299 training samples and 144 testing samples. All methods are evaluated with the same sampled splits for a fair comparison.

Experimental Settings. For both datasets, visible images, thermal images, and semantic labels are resized to 512×512 for training. We use the AdamW[38] optimizer for all training stages of the VAE and diffusion models. Random horizontal flipping is adopted as the basic data augmentation strategy. All compared methods follow the same data preprocessing pipeline and training settings.

4.2 Main Comparison with Existing Pipelines

To the best of our knowledge, text-driven generation of aligned VIS-IR-Label triplets from limited paired training data has not been explicitly studied before. Therefore, we construct three representative cascaded alternatives for comparison, namely Seq-Cascade, JointLabel-Cascade, and TriCond-Cascade. To ensure fairness, the text-to-image generation module and the joint generation module in the three cascaded schemes are both implemented based on the UniDiffuser[34] architecture, while the Visible-to-Infrared image translation module is implemented based on DiffV2IR[21].

Quantitative Results Table 1 compares our method with three representative cascaded pipelines on the SemanticRT and PST900 datasets. On the 5% SemanticRT setting, where only 342 real training pairs are available, adding an equal number of synthetic triplets generated by UniTriGen consistently improves all downstream RGB-T segmentation models. Similar trends can be observed on the 50% PST900 setting, where 299 synthetic triplets are added to 299 real training pairs. UniTriGen improves the raw-data baseline from 78.51 to 83.96, 74.96 to 79.31, 85.86 to 87.06, and 86.42 to 87.29 across the four downstream architectures, respectively. These results demonstrate that UniTriGen-generated triplets provide effective, model-agnostic data augmentation with limited paired supervision. Compared with the cascaded alternatives, UniTriGen achieves consistently superior performance in both the synthetic-only and real-plus-synthetic settings. When combined with real data, UniTriGen consistently achieves the highest mIoU among all compared methods across different downstream models. On PST900, the advantage is more pronounced. These consistent improvements indicate that cascaded pipelines, although able to assemble VIS-IR-Label triplets, suffer from accumulated errors and insufficient joint cross-modal constraints. In contrast, UniTriGen directly models the joint distribution of VIS, IR, and Label within a unified diffusion process, leading to better spatial alignment, semantic consistency, and downstream training utility.

Qualitative Results Figure 3 visualizes the VIS-IR-Label triplets generated by UniTriGen on SemanticRT and PST900. Across diverse scenes and classes, UniTriGen produces aligned triplets with clear spatial alignment and semantic consistency among the three modalities. The generated VIS images preserve realistic scene appearance and structural layouts, while the IR images exhibit

modality-specific thermal characteristics, such as salient human targets and weakened texture responses, rather than simply copying visible-domain patterns. Meanwhile, the generated labels are well aligned with object boundaries and remain accurate for small or thin structures, such as poles, car stop, drills, and fire extinguishers. Notably, UniTriGen can distinguish visually or semantically similar classes, including Tricycle, Motorcycle, and Bike, as well as Motorcyclist, Bicyclist, and Person. These results indicate that the proposed unified generation framework can synthesize high-quality VIS-IR-Label triplets with strong cross-modal coherence.

Figure 4 provides a qualitative comparison between UniTriGen and the cascaded variants. Overall, the cascaded pipelines show evident cross-modal inconsistency due to their multi-stage generation process. In JointLabel-Cascade and TriCond-Cascade, once a class is missed in the generated label, such as the person in the dark region, the corresponding object is also absent or weakened in the synthesized IR image, indicating that errors are propagated across stages. Moreover, JointLabel-Cascade sometimes produces IR results that resemble appearance-level tone transfer rather than physically plausible thermal imaging; for example, the covered parked car exhibits unrealistic thermal responses. Seq-Cascade further suffers from noisy semantic predictions, since its final labels heavily depend on the quality of the previously generated VIS and IR images. In contrast, UniTriGen directly models VIS, IR, and Label as a unified triplet, producing more consistent object presence, more realistic IR modality characteristics, and better-aligned semantic labels.

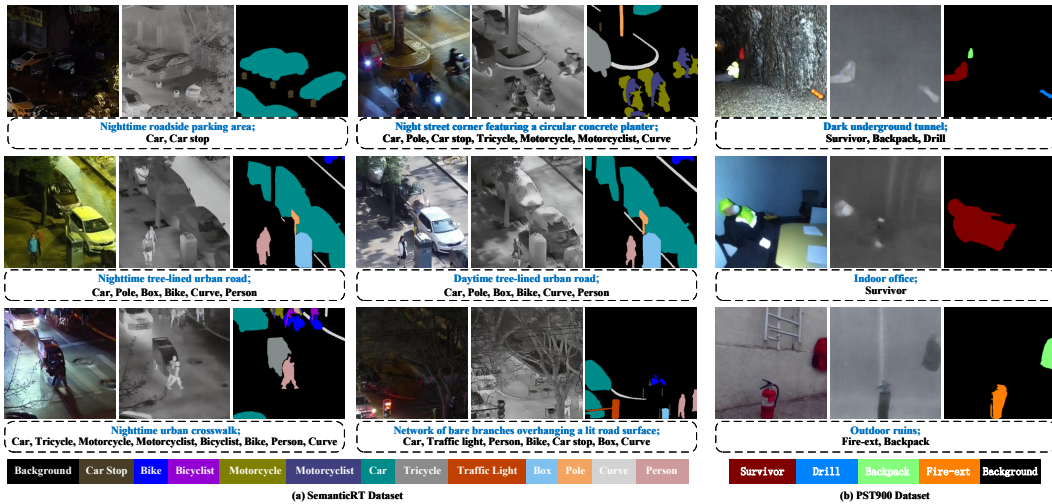


Figure 3: Visualization of UniTriGen generation results on the SemanticRT dataset and PST900 dataset. The text prompt consists of `scene` and categories.

4.3 Ablation Studies

Table 2 presents the ablation study results of the proposed components in UniTriGen. Without incorporating synthetic data, the M-SpecGene [39] method achieves 69.38 on the original 5% SemanticRT setting and 74.96 on the original 50% PST900 setting. When applying the unified triplet generation mechanism, the performance increases to 70.79 and 78.79 on SemanticRT and PST900, respectively, demonstrating that jointly modeling VIS, IR, and label triplets provides an effective foundation for cross-modal data generation. Building upon this mechanism, introducing SBCA Few-Shot Sampling further improves the performance to 71.57 on SemanticRT and 79.31 on PST900, yielding gains of 0.78 and 0.52 points, respectively. These results indicate that scene-balanced and class-aware sampling can better exploit limited paired data and alleviate the class-imbalance issue under few-shot settings. Overall, the ablation results validate the effectiveness and complementarity of the proposed generation and sampling strategies.

4.4 Extend Analysis

Performance under Different Real-data Ratios While our main experiments use 5% of SemanticRT and 50% of PST900, UniTriGen is not tied to a fixed real-data ratio. To evaluate its robustness across data scales, we train UniTriGen with different ratios of paired real triplets and add the generated triplets to the corresponding real training sets for downstream evaluation. As shown in

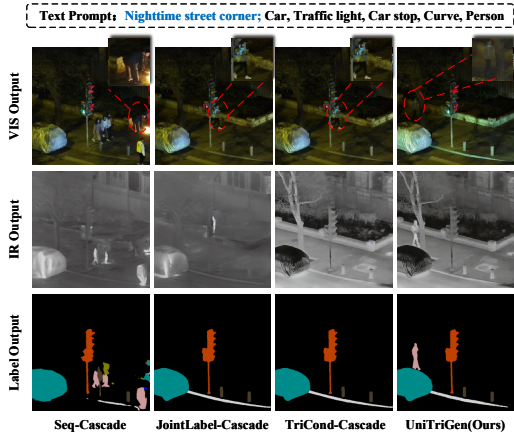


Figure 4: Qualitative comparison of different VIS-IR-Label generation pipelines on the SemanticRT dataset.

Method Components			Downstream Performance	
UniTriGen Mechanism	SBCA Few-Shot Sampling		5% SemanticRT	50% PST900
✓			70.79	78.79
✓	✓		71.57	79.31

Table 2: Ablation results for different components of the proposed method, where “UniTriGen Mechanism” denotes the unified triplet generation mechanism.

Ratio	SemanticRT			PST900		
	Real	Real+Syn		Ratio	Real	Real+Syn
5%	69.38	71.57		50%	74.96	79.31
10%	71.65	73.62		75%	76.52	80.19
25%	77.35	78.28		100%	79.71	81.92

Table 3: Performance comparison under different real-data ratios.

Datasets	Scaling with Synthetic Data Size			
	1Real	1Real:1Syn	1Real:10Syn	1Real:20Syn
5% SemanticRT	69.38	71.57(+2.19↑)	72.00(+2.62↑)	72.13(+2.75↑)
50% PST900	74.96	79.31(+4.35↑)	80.38(+5.42↑)	81.54(+6.58↑)

Table 4: Comparison of downstream performance under different real-to-synthetic data ratios.

Table 3, UniTriGen consistently improves M-SpecGene [39] across all tested ratios, demonstrating its effectiveness under varying amounts of paired supervision. Notably, even with only 342 real triplets from 5% SemanticRT and 299 real triplets from 50% PST900, UniTriGen still produces synthetic triplets that improve downstream performance. This indicates that UniTriGen does not rely on large-scale paired supervision, which is crucial for RGB-T scenarios where aligned VIS-IR-Label triplets are scarce.

Scaling with Synthetic Data Size We further examine the impact of synthetic data scale on downstream performance. As shown in Table 4, under the 5% SemanticRT setting, increasing the real-to-synthetic data ratio from 1:1 to 1:10 and 1:20 steadily improves the mIoU of M-SpecGene[39] from 71.57 to 72.00 and 72.13, corresponding to gains of 2.19, 2.62, and 2.75 relative to the real-only baseline, respectively. Similar trends can be observed on the 50% PST900 setting. These trends indicate that the aligned triplets generated by UniTriGen can consistently benefit downstream training as more synthetic data are incorporated. Compared with relying solely on limited real samples, larger synthetic datasets provide richer scene layouts, object appearances, and cross-modal correspondences, thereby leading to improved few-shot RGB-T semantic segmentation performance.

5 Conclusion

In this paper, we propose UniTriGen, a text-driven VIS-IR-Label triplet generation framework for scenarios with only a limited number of paired VIS-IR-Label triplets available for training. UniTriGen directly models visible images, infrared images, and semantic labels within a unified generation process, thereby alleviating the difficulty of cascaded generation paradigms in maintaining cross-modal consistency. Specifically, the proposed Unified Triplet Generation Mechanism jointly encodes the three modalities into a shared latent space, models the concatenated latent representation through a diffusion process, and incorporates lightweight modality-specific residual adapters to preserve both cross-modal consistency and modality-specific fidelity. In addition, to mitigate generation bias caused by imbalanced scene and class distributions, we design an SBCA few-shot sampling strategy, which encourages a more balanced sampling distribution and improves the diversity of generated triplets. Extensive experiments on SemanticRT and PST900 demonstrate the effectiveness of UniTriGen in generating training-ready VIS-IR-Label triplets and improving downstream performance.

References

- [1] Xingsong Ye, Yongkun Du, Yunbo Tao, and Zhineng Chen. Textssr: diffusion-based data synthesis for scene text recognition. In *Proceedings of the IEEE/CVF International Conference on Computer Vision*, pages 17464–17473, 2025.
- [2] Chenyang Liu, Keyan Chen, Rui Zhao, Zhengxia Zou, and Zhenwei Shi. Text2earth: Unlocking text-driven remote sensing image generation with a global-scale dataset and a foundation model. *IEEE Geoscience and Remote Sensing Magazine*, 2025.
- [3] Weijia Wu, Yuzhong Zhao, Hao Chen, Yuchao Gu, Rui Zhao, Yefei He, Hong Zhou, Mike Zheng Shou, and Chunhua Shen. Datasetdm: Synthesizing data with perception annotations using diffusion models. *Advances in Neural Information Processing Systems*, 36:54683–54695, 2023.
- [4] Quang Nguyen, Truong Vu, Anh Tran, and Khoi Nguyen. Dataset diffusion: Diffusion-based synthetic data generation for pixel-level semantic segmentation. *Advances in Neural Information Processing Systems*, 36:76872–76892, 2023.
- [5] Dong Zhao, Qi Zang, Shuang Wang, Nicu Sebe, and Zhun Zhong. Pseudo-sd: pseudo controlled stable diffusion for semi-supervised and cross-domain semantic segmentation. In *Proceedings of the IEEE/CVF International Conference on Computer Vision*, pages 22393–22403, 2025.
- [6] Haoyu Wang, Lei Zhang, Wenrui Liu, Dengyang Jiang, Wei Wei, and Chen Ding. Jodiffusion: Jointly diffusing image with pixel-level annotations for semantic segmentation promotion. In *Proceedings of the AAAI Conference on Artificial Intelligence*, volume 40, pages 9775–9783, 2026.
- [7] Robin Rombach, Andreas Blattmann, Dominik Lorenz, Patrick Esser, and Björn Ommer. High-resolution image synthesis with latent diffusion models. In *Proceedings of the IEEE/CVF conference on computer vision and pattern recognition*, pages 10684–10695, 2022.
- [8] Lvmin Zhang, Anyi Rao, and Maneesh Agrawala. Adding conditional control to text-to-image diffusion models. In *Proceedings of the IEEE/CVF international conference on computer vision*, pages 3836–3847, 2023.
- [9] Nataniel Ruiz, Yuanzhen Li, Varun Jampani, Yael Pritch, Michael Rubinstein, and Kfir Aberman. Dreambooth: Fine tuning text-to-image diffusion models for subject-driven generation. In *Proceedings of the IEEE/CVF conference on computer vision and pattern recognition*, pages 22500–22510, 2023.
- [10] Black Forest Labs, Stephen Batifol, Andreas Blattmann, Frederic Boesel, Saksham Consul, Cyril Diagne, Tim Dockhorn, Jack English, Zion English, Patrick Esser, et al. Flux. 1 kontext: Flow matching for in-context image generation and editing in latent space. *arXiv preprint arXiv:2506.15742*, 2025.
- [11] Dustin Podell, Zion English, Kyle Lacey, Andreas Blattmann, Tim Dockhorn, Jonas Müller, Joe Penna, and Robin Rombach. Sdxl: Improving latent diffusion models for high-resolution image synthesis. In *The Twelfth International Conference on Learning Representations*.
- [12] Weijia Wu, Yuzhong Zhao, Mike Zheng Shou, Hong Zhou, and Chunhua Shen. Diffumask: Synthesizing images with pixel-level annotations for semantic segmentation using diffusion models. In *Proceedings of the IEEE/CVF International Conference on Computer Vision*, pages 1206–1217, 2023.
- [13] Hao Tang, Siyue Yu, Jian Pang, and Bingfeng Zhang. A training-free synthetic data selection method for semantic segmentation. In *Proceedings of the AAAI Conference on Artificial Intelligence*, volume 39, pages 7229–7237, 2025.
- [14] Tianhe Ren, Shilong Liu, Ailing Zeng, Jing Lin, Kunchang Li, He Cao, Jiayu Chen, Xinyu Huang, Yukang Chen, Feng Yan, et al. Grounded sam: Assembling open-world models for diverse visual tasks. *arXiv preprint arXiv:2401.14159*, 2024.
- [15] Alec Radford, Jong Wook Kim, Chris Hallacy, Aditya Ramesh, Gabriel Goh, Sandhini Agarwal, Girish Sastry, Amanda Askell, Pamela Mishkin, Jack Clark, et al. Learning transferable visual models from natural language supervision. In *International conference on machine learning*, pages 8748–8763. PmLR, 2021.
- [16] Hanrong Ye, Jason Kuen, Qing Liu, Zhe Lin, Brian Price, and Dan Xu. Seggen: Supercharging segmentation models with text2mask and mask2img synthesis. In *European Conference on Computer Vision*, pages 352–370. Springer, 2024.

- [17] Lihe Yang, Xiaogang Xu, Bingyi Kang, Yinghuan Shi, and Hengshuang Zhao. Freemask: Synthetic images with dense annotations make stronger segmentation models. *Advances in Neural Information Processing Systems*, 36:18659–18675, 2023.
- [18] Haoxuan Zhang, Wenju Cui, Yuzhu Cao, Tao Tan, Jie Liu, Yunsong Peng, and Jian Zheng. Paired image generation with diffusion-guided diffusion models. In *International Conference on Medical Image Computing and Computer-Assisted Intervention*, pages 371–381, 2025.
- [19] Wenbo Dai, Lijing Lu, and Zhihang Li. Diffusion-based synthetic data generation for visible-infrared person re-identification. In *Proceedings of the AAAI Conference on Artificial Intelligence*, volume 39, pages 11185–11193, 2025.
- [20] Fangyuan Mao, Jilin Mei, Shun Lu, Fuyang Liu, Liang Chen, Fangzhou Zhao, and Yu Hu. Pid: Physics-informed diffusion model for infrared image generation. *Pattern Recognition*, 169:111816, 2026.
- [21] Lingyan Ran, Lidong Wang, Guangcong Wang, Peng Wang, and Yanning Zhang. Diffv2ir: visible-to-infrared diffusion model via vision-language understanding. *arXiv preprint arXiv:2503.19012*, 2025.
- [22] HyeongJoo Hwang, Geon-Hyeong Kim, Seunghoon Hong, and Kee-Eung Kim. Variational interaction information maximization for cross-domain disentanglement. *Advances in Neural Information Processing Systems*, 33:22479–22491, 2020.
- [23] Diederik P Kingma and Max Welling. Auto-encoding variational bayes. *arXiv preprint arXiv:1312.6114*, 2013.
- [24] Phillip Isola, Jun-Yan Zhu, Tinghui Zhou, and Alexei A Efros. Image-to-image translation with conditional adversarial networks. In *Proceedings of the IEEE conference on computer vision and pattern recognition*, pages 1125–1134, 2017.
- [25] Ting-Chun Wang, Ming-Yu Liu, Jun-Yan Zhu, Andrew Tao, Jan Kautz, and Bryan Catanzaro. High-resolution image synthesis and semantic manipulation with conditional gans. In *Proceedings of the IEEE conference on computer vision and pattern recognition*, pages 8798–8807, 2018.
- [26] Jun-Yan Zhu, Taesung Park, Phillip Isola, and Alexei A Efros. Unpaired image-to-image translation using cycle-consistent adversarial networks. In *Proceedings of the IEEE international conference on computer vision*, pages 2223–2232, 2017.
- [27] Dong-Guw Lee, Myung-Hwan Jeon, Younggun Cho, and Ayoung Kim. Edge-guided multi-domain rgb-to-tir image translation for training vision tasks with challenging labels. In *2023 IEEE International Conference on Robotics and Automation (ICRA)*, pages 8291–8298. IEEE, 2023.
- [28] Mehmet Akif Özkanoğlu and Sedat Ozer. Infragan: A gan architecture to transfer visible images to infrared domain. *Pattern Recognition Letters*, 155:69–76, 2022.
- [29] Zonghao Han, Shun Zhang, Yuru Su, Xiaoning Chen, and Shaohui Mei. Dr-avit: Toward diverse and realistic aerial visible-to-infrared image translation. *IEEE Transactions on Geoscience and Remote Sensing*, 62:1–13, 2024.
- [30] Qiyang Sun, Xia Wang, Changda Yan, and Xin Zhang. Vq-infratrans: A unified framework for rgb-ir translation with hybrid transformer. *Remote Sensing*, 15(24):5661, 2023.
- [31] Chong Mou, Xintao Wang, Liangbin Xie, Yanze Wu, Jian Zhang, Zhongang Qi, and Ying Shan. T2i-adapter: Learning adapters to dig out more controllable ability for text-to-image diffusion models. In *Proceedings of the AAAI conference on artificial intelligence*, volume 38, pages 4296–4304, 2024.
- [32] Haoyang Chen, Jing Zhang, Hebaixu Wang, Shiqin Wang, Pohsun Huang, Jiayuan Li, Haonan Guo, Di Wang, Zheng Wang, and Bo Du. Any2any: Unified arbitrary modality translation for remote sensing. *arXiv preprint arXiv:2603.04114*, 2026.
- [33] Xi Yang, Haoyuan Shi, Ziyun Li, Maoying Qiao, Fei Gao, and Nannan Wang. S 3 oil: Semi-supervised sar-to-optical image translation via multi-scale and cross-set matching. *IEEE Transactions on Image Processing*, 2025.
- [34] Fan Bao, Shen Nie, Kaiwen Xue, Chongxuan Li, Shi Pu, Yaole Wang, Gang Yue, Yue Cao, Hang Su, and Jun Zhu. One transformer fits all distributions in multi-modal diffusion at scale. In *International Conference on Machine Learning*, pages 1692–1717. PMLR, 2023.
- [35] Bolei Zhou, Agata Lapedriza, Aditya Khosla, Aude Oliva, and Antonio Torralba. Places: A 10 million image database for scene recognition. *IEEE Transactions on Pattern Analysis and Machine Intelligence*, 2017.

- [36] Wei Ji, Jingjing Li, Cheng Bian, Zhicheng Zhang, and Li Cheng. Semanticrt: A large-scale dataset and method for robust semantic segmentation in multispectral images. In *Proceedings of the 31st ACM International Conference on Multimedia*, pages 3307–3316, 2023.
- [37] Shreyas S Shivakumar, Neil Rodrigues, Alex Zhou, Ian D Miller, Vijay Kumar, and Camillo J Taylor. Pst900: Rgb-thermal calibration, dataset and segmentation network. In *2020 IEEE international conference on robotics and automation (ICRA)*, pages 9441–9447. IEEE, 2020.
- [38] Ilya Loshchilov and Frank Hutter. Decoupled weight decay regularization. *arXiv preprint arXiv:1711.05101*, 2017.
- [39] Kailai Zhou, Fuqiang Yang, Shixian Wang, Bihan Wen, Chongde Zi, Linsen Chen, Qiu Shen, and Xun Cao. M-specgene: Generalized foundation model for rgbt multispectral vision. In *Proceedings of the IEEE/CVF International Conference on Computer Vision*, pages 7861–7872, 2025.
- [40] Zifu Wan, Pingping Zhang, Yuhao Wang, Silong Yong, Simon Stepputtis, Katia Sycara, and Yaqi Xie. Sigma: Siamese mamba network for multi-modal semantic segmentation. In *2025 IEEE/CVF Winter Conference on Applications of Computer Vision (WACV)*, pages 1734–1744. IEEE, 2025.
- [41] Jinfu Liu, Hong Liu, Xia Li, Jiale Ren, and Xinhua Xu. Milnet: Multiplex interactive learning network for rgb-t semantic segmentation. *IEEE Transactions on Image Processing*, 2025.